Neutral current cross sections at high x

Y. Ning on behalf of the ZEUS collaboration

DESY ZEUS Columbia, Notke Str. 85, 22607 Hamburg, Germany
Pupin 5283, 538 W. 120th Str., New York, NY 10027, USA

Abstract. A new method is employed to measure the neutral current cross section up to Bjorken-x values equal to one with the ZEUS detector at HERA using an integrated luminosity of 65 pb^{-1}. Cross sections have been extracted for $Q^2 > 576$ GeV^2 and are compared to predictions using different parton density functions (PDFs). The data produce new constraints on the PDFs at the high values of x.

Keywords: neutral current cross section, high x, ZEUS, HERA
PACS: 13.60.Hb

INTRODUCTION

The electron-proton deep inelastic scattering (DIS) cross section is written in terms of the proton structure functions, which can be writen in terms of PDFs and electroweak parameters. The PDFs are found to decrease very quickly for $x \geq 0.3$. The form of the PDF is typically parameterized as $(1-x)^{\eta}$ near $x \to 1$, as expected from counting rule arguments [1], and this form follows the data quite well [2, 3]. However, a direct confrontation with data has not been possible to date for $x \to 1$ due to limitations in beam energies and measurement techniques. The highest measured points in the DIS regime are for $x = 0.75$ [4]. Data at higher x exist [5, 6] but these are in the resonance production region and cannot be easily interpreted in terms of parton distributions. The highest x value for HERA structure function data is $x = 0.65$.

EXPERIMENTAL SETUP AND PROPOSED METHOD

At HERA, proton beams of 920 GeV (820 GeV prior to 1998), collide with either electron or positron beams of 27.5 GeV. ZEUS is a multipurpose detector described in detail elsewhere [7]. A schematic depiction of the ZEUS detector is given in Fig. 1. The components most relevant in this analysis are the uranium–scintillator calorimeter (CAL) [8–11], and the central tracking detector (CTD) [12–14]

Figure 1 includes a schematic depiction of a NC event: a scattered electron and a jet are outlined in the CAL, while the proton remnant largely disappears down the forward beam pipe. E'_e and E_{jet} are the energies of the scattered electron and jet; θ_e and θ_{jet} are the polar angles with respect to the proton beam direction. As x increases, the jet is boosted in the forward direction and θ_{jet} decreases. When x is too high, a part of the jet is lost in the beam pipe. The value of x at which this occurs is Q^2 dependent: the x values for which jets are well contained increases as Q^2 increases. At the Q^2 values considered in

this analysis, the scattered electron is at large angles and well contained in the detector. The new method employed in this analysis combines electron and jet information to

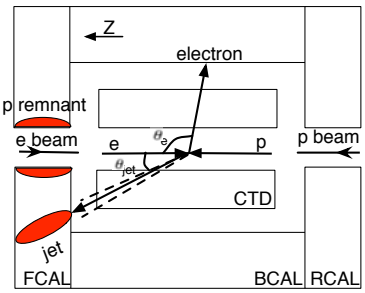

Figure 1. A schematic depiction of the ZEUS detector with the main components used in this analysis labeled. Also shown is a typical topology for events studied in this analysis. The electron is scattered at large angles and is reconstructed using the central tracking chamber (CTD) and the barrel calorimeter (BCAL), while the scattered jet is typically reconstructed in the forward calorimeter (FCAL). The jet of particles from the proton remnant largely disappears down the beam pipe.

allow a measurement of the differential cross section up to $x = 1$. Events are first sorted into Q^2 bins using information from the electron only: $Q^2 = 2E_eE'_e(1+\cos\theta_e)$, where E_e is the electron beam energy. The jet information is then used to calculate x from E_{jet} and θ_{jet} for events with a well reconstructed jet. These events are sorted into x bins to allow a measurement of the double differential cross section $d^2\sigma/dxdQ^2$. Events with no jet reconstructed within the fiducial volume are assumed to come from high x and are collected in a bin with $x_{Edge} < x < 1$. Since these bins are generally large and the form of the PDF is not well known in this region, an integrated cross section is calculated; $\int_{x_{Edge}}^{1}(d^2\sigma/dxdQ^2)dx$. Events with more than one high energy jet are discarded.

The features of this method are:

- good resolution in Q^2 for all x;
- good resolution in x in events where a jet can be reconstructed;
- cross section measurements possible up to $x = 1$.

DATA SET

The measurement is based on the data collected by ZEUS from 1999 to 2000. The data corresponds to an integrated luminosity of 65.1 pb^{-1} for e^+p collisions. Events with high energy electron with strict fiducial cuts and zero or one jet with high transverse energy and $\theta_{jet} > 0.12$ rad are selected. The simulated MC events were used to evaluate the efficiency for the event selection and to determine the accuracy of the kinematic reconstruction. A sufficient number of events was used to ensure the statistical uncertainties from the MC samples were negligible compared to those in the data.

MC distributions are compared with those from the data. The MC distributions have been normalized to the measured luminosity. Good agreement between data and MC simulation is observed for both zero and one jet events, and there is no indication of

residual backgrounds. For zero jet events, about 10 % more data events are observed than expected in the simulation.

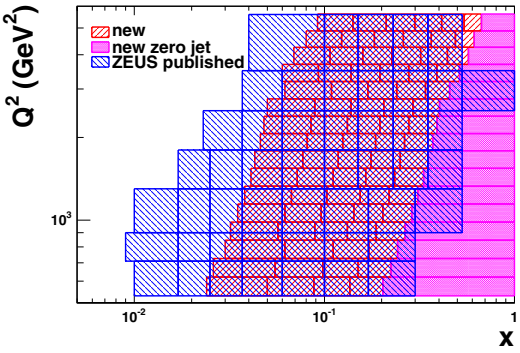

Figure 2. Definition of the bins as used in this analysis. The magenta bins extending to $x = 1$ are for the zero jet events. The blue bins show the bin structure ZEUS published [15].

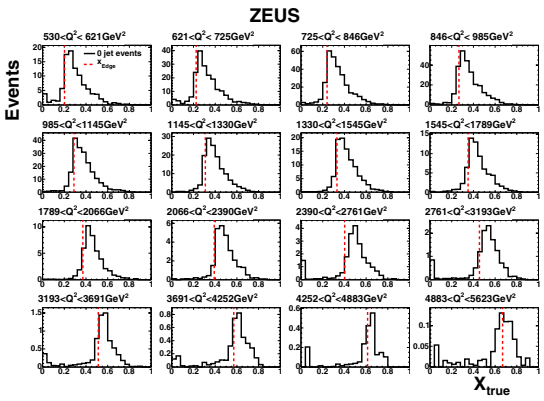

Figure 3. The true x distribution from NC MC simulations for zero jet events in different Q^2 bins as indicated in the plots. The dashed lines represent the lower edge of the bins, x_{Edge}. The MC distributions are normalized to the luminosity of the data.

The bin definitions used in this analysis are given in Fig. 2. The bin widths for the double differential cross section measurements were chosen to correspond to three times the resolution of the reconstructed kinematic variables and the definition of the x bin boundaries vary with Q^2 since x_{Edge} is strongly Q^2 dependent. The x resolution of the new method is better than that of the double angle method (DA) which is usually used by ZEUS, which allows a more accurate measurement and smaller bins as shown in the figure.

The MC simulation was used to study the x distribution of the zero jet events which are assigned to the highest x bin. Figure 3 shows the true x distribution for these MC events in different Q^2 bins. As can be seen in this figure, the zero jet events originate predominantly from the interval $x_{Edge} < x < 1$. The purity in these bins is high and comparable to the purity in mid-x bins.

RESULTS AND CONCLUSION

The measured cross sections are shown in Fig. 4 and compared to SM expectations at NLO using the CTEQ6D parton distributions [16]. The double differential cross sections are represented by solid points, and generally agree well with the expectations. The cross section in the highest x bin is given as

$$\frac{1}{1-x_{Edge}} \int_{x_{Edge}}^{1} \frac{d^2\sigma}{dx dQ^2} dx \ .$$

In this bin, the expected cross section is drawn as a horizontal line, while the measured cross section is displayed as the open symbol. The measured data is plotted at the center of the bin, but it should be understood to be an integrated cross section for the bin.

The error bars represent the quadratic sum of the systematic and statistical uncertainties, where the statistical uncertainties are calculated from the square root of the number of observed events.

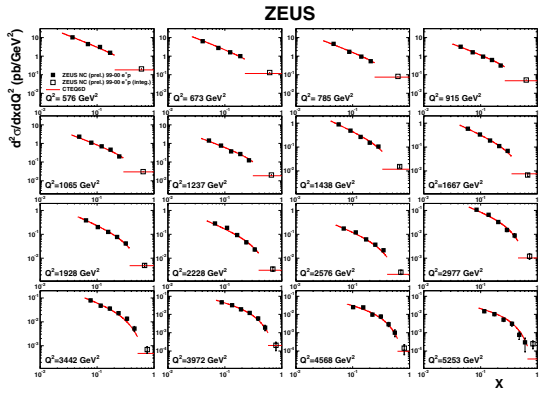

Figure 4. The double differential cross section (solid squares) and the integral of the double differential cross section divided by the bin width (open squares) compared to the Standard Model (SM) expectations evaluated using CTEQ6D PDFs (lines). The inner error bars show the statistical uncertainty, while the outer ones show the statistical and systematic uncertainties added in quadrature.

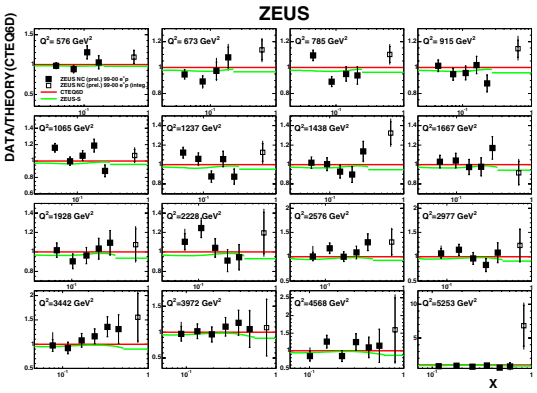

Figure 5. Ratio of the double differential cross section (solid squares) and the integral of the double differential cross section divided by x bin width (open squares) to the SM expectation evaluated using the CTEQ6D PDFs. The inner error bars show the statistical uncertainty, while the outer ones show the statistical and systematic uncertainties added in quadrature. The ratio of the expectations using the CTEQ6D PDFs to those using the ZEUS-S predictions is shown as the green (grey) lines.

The ratio of the measured cross sections to SM expectation using the CTEQ6D PDFs is shown in Fig. 5. The ratio of the expectation using the CTEQ6D PDFs to that using ZEUS-S PDFs [17] is also shown. The measured double differential cross sections generally agree well with both sets of expectations. For the highest x bins, which are in previously unmeasured kinematic ranges, the data has a tendency to lie above the expectations. These data are expected to have an impact on the extraction of the PDFs at the highest values of x, and via sum rules, also the PDFs at smaller x.

REFERENCES

1. R. Blankenbecler, and S. Brodsky, *Phys. Rev.*, **D 10**, 2973 (1974).
2. A. Martin, et al., NNLO global parton analysis (2002), `hep-ph/0201127`.
3. J. Pumplin, et al., New generation of parton distributions with uncertainties from global QCD analysis (2002), `hep-ph/0201195`.
4. A. Benvenuti, et al., *Phys. Lett.*, **B 223**, 485 (1989).
5. L. Whitlow, et al., *Phys. Lett.*, **B 282**, 475 (1992).
6. M. Osipenko, et al., *Phys. Rev.*, **D 67**, 092001 (2003).
7. The ZEUS detector, Status Report (unpublished), DESY (1993).
8. M. Derrick, et al., *NIM*, **A 309**, 77 (1991).
9. A. Andresen, et al., *NIM*, **A 309**, 101 (1991).
10. A. Caldwell, et al., *NIM*, **A 321**, 356 (1992).
11. A. Bernstein, et al., *NIM*, **A 336**, 23 (1993).
12. N. Harnew, et al., *NIM*, **A 279**, 290 (1989).
13. B. Foster, et al., *NPPS*, **B 32**, 181 (1993).

14. B. Foster, et al., *NIM*, **A 338**, 254 (1994).
15. S. C. ZEUS Collab., et al., *Phys. Rev.*, **D 70**, 052001 (2004), hep-ex/0401003.
16. J. Pumplin, et al., *JHEP*, **0207**, 012 (2002).
17. S. Chekanov, et al., *Phys. Rev.*, **D 67**, 12007 (2003).